International Journal of Heat and Mass Transfer 52 (2009) 3850–3856

Contents lists available at ScienceDirect

International Journal of Heat and Mass Transfer

journal homepage: www.elsevier.com/locate/ijhmt

# Buoyancy-induced flow in an open-ended cavity: Assessment of a similarity solution and of numerical simulation models

S.K.S. Boetcher [a], E.M. Sparrow [b,*]

[a] Department of Mechanical and Energy Engineering, Center for Advanced Scientific Computing and Modeling (CASCaM), University of North Texas, Denton, TX 76207-7102, USA
[b] Laboratory for Heat Transfer Practice, Department of Mechanical Engineering, University of Minnesota, Minneapolis, MN 55455-0111, USA

ARTICLE INFO

*Article history:*
Received 10 October 2008
Received in revised form 12 October 2008
Accepted 12 October 2008
Available online 7 April 2009

*Keywords:*
Buoyant flow
Open-ended cavity
Similarity solution
Numerical simulation
Nusselt numbers

ABSTRACT

The buoyancy-induced flow in a horizontal open-ended cavity has been investigated from three perspectives: (a) assessment of the validity of an existent similarity solution, (b) computational issues relevant to numerical simulation, and (c) obtainment and presentation of results of practical utility. Parameter ranges were sought within which the similarity solution might be valid, but no such ranges could be identified. The inapplicability of the similarity model may be attributed to the neglect of the streamwise second derivatives in the governing conservation equations and to the model's inability to accommodate boundary conditions at the opening of the channel. The numerical issues that were dealt with included the proper extension of the solution domain into the far field external to the channel, the appropriate boundary conditions on the surfaces of the extended domain, and meshing to achieve high accuracy. Local Nusselt numbers and their variation along the walls of the channel are presented.



## 1. Introduction

The past quarter century has seen an evolving literature dealing with a pair of closely related natural convection problems involving the buoyancy-driven interaction of fluid in a semi-confined space with fluid in an extensive external space. One of these problems, often termed the open-ended cavity, is a horizontal parallel-walled channel that is open at both ends and which interacts with an extensive space adjacent to the respective ends. The second problem is either called the partially open cavity or the open cavity. It consists of a horizontal channel closed at one end and open to an extensive space at its other end. The applications of these fundamental problems include electronic equipment cooling, fire incidents in internal spaces, chemical vapor deposition systems, solar collectors, and nuclear reactor incidents.

An early and truly seminal contribution to this problem area is that of Bejan [1]. Following a model for buoyant flow in a vertical, open thermosyphon due to Lighthill [2], Bejan developed a solution for the fluid flow and heat transfer within an open cavity without having to take account of the fluid in the space external to the cavity. The solution was actually a similarity solution, generically related to the celebrated Blasius solution for forced convection flow over a flat plate. In both these cases, the basic two-dimensional partial differential equations which govern the respective problems are reduced to ordinary differential equations by a similarity transformation.

Notwithstanding the elegance of similarity solutions, it is widely understood that they have numerous practical limitations which restrict their applicability. For instance, for the venerable Blasius flat-plate problem, there are both Reynolds and Prandtl number (for heat transfer) limitations in addition to the plate thinness requirement.

One of the goals of the present investigation is to define the parametric ranges of applicability of the Bejan similarity solution for the open cavity. The dimensionless parameters that characterize the problem are the Rayleigh number, Prandtl number, and the cavity aspect ratio. This goal will be achieved by a benchmark-quality numerical simulation of the problem.

Another goal of this work is to deal definitively with three issues which have impacted prior numerical simulations of the problem. They are: (a) the extension of the solution domain into the external space adjacent to the cavity opening(s), (b) the boundary conditions applied to the surfaces of the extended domain, and (c) the mesh density used in the numerical solutions.

The extended solution domains used by Penot [3] and by Chan and Tien [4] were inappropriately small. In addition, the grid density (800 and 2000 elements, respectively) is insufficient when judged by current standards. In addition, the boundary conditions applied to the surfaces of the extended domain do not express reality. Vafai and Ettefagh [5] demonstrated the importance of a large extended solution domain. The boundary conditions applied to the surfaces of the extended domain are those presently regarded as

* Corresponding author. Tel.: +1 612 625 5502.
*E-mail address:* esparrow@umn.edu (E.M. Sparrow).

0017-9310/$ - see front matter © 2009 Elsevier Ltd. All rights reserved.
doi:10.1016/j.ijheatmasstransfer.2008.10.035

**Nomenclature**

| | |
|---|---|
| $c_p$ | specific heat |
| $Gr$ | Grashof number, Eq. (2) |
| $g$ | acceleration of gravity |
| $H$ | height of cavity |
| $h$ | heat transfer coefficient, Eq. (9) |
| $k$ | thermal conductivity |
| $L$ | length of channel |
| $Nu$ | Nusselt number, Eq. (10) |
| $n$ | surface normal |
| $P$ | dimensionless pressure, Eq. (1) |
| $p$ | pressure |
| $Pr$ | Prandtl number, Eq. (2) |
| $q$ | local heat flux |
| $Ra$ | Rayleigh number, Eq. (2) |
| $T$ | temperature |
| $T_w$ | wall temperature |
| $T_\infty$ | far-field temperature |
| $U$, $V$ | dimensionless velocities, Eq. (1) |
| $u$, $v$ | velocity components |
| $X$, $Y$ | dimensionless Cartesian coordinates, Eq. (1) |
| $x$, $y$ | Cartesian coordinates |
| *Greek* | |
| $\beta$ | coefficient of thermal expansion |
| $\theta$ | dimensionless temperature, Eq. (1) |
| $\mu$ | viscosity |
| $\nu$ | kinematic viscosity |
| $\rho$ | density |
| $\rho_\infty$ | density in the far field |
| $\tau$ | temperature profile shape, Eq. (8) |
| $\phi'$ | velocity profile shape, Eq. (7) |
| *Subscript* | |
| *pen* | penetration depth |

applicable to outflow boundaries, and the mesh density was not specified. Follow-on papers by Khanafer and Vafai [6,7] also imposed outflow conditions on the boundaries of the extended solution domain. These authors also attempted to find a set of fictive boundary conditions to be applied at the open end of the cavity whose use would obviate the need for an extended solution domain. However, according to Icoz and Jaluria [8], these fictive boundary conditions are applicable only to specific geometries and limited flow conditions.

The focus of the aforementioned Icoz–Jaluria paper was an open-ended channel with heat sources protruding into the channel. The solution domain was not extended into the space external to the channel. Very recently, Andreozzi et al. [9] numerically investigated an open-ended cavity having thermal boundary conditions different from those of preceding studies. An extended solution domain of unspecified size was used, but the schematic diagram of the problem, if to scale, suggests possible sizewise insufficiency. The boundary conditions applied at the surfaces of the extended domain totally precluded vertical flow there.

The simulation model used here eliminates all of the issues of uncertainty that were identified in the preceding paragraphs and, thereby, provides results of impeccable accuracy.

## 2. The solution domain and boundary conditions

A schematic diagram of the open cavity and of the adjacent fluid environment is exhibited in Fig. 1. The diagram also shows, as a dashed-line closed contour, the solution domain within which the numerical simulations are to be performed. Consistent with the two-dimensional model displayed in the figure, the coordinates are $x$ and $y$, and the length and height dimensions of the cavity are $L$ and $H$, respectively. The cavity aspect ratio $AR$ is equal to $L/H$. The extended solution domain, the rectangle $ABCDA$, is much larger in size than the cavity proper in accordance with the concerns discussed earlier. In particular, the width and total height of the extended domain are $10H$ and $18H$, respectively.

The boundary conditions at the walls of the cavity proper were selected to facilitate the assessment of the validity of the similarity solution of [1]. The no-slip and impermeability conditions require that the velocity components $u$ and $v$ are zero on all the cavity walls. In addition, all of the walls of the cavity are isothermal at a common temperature $T_w$.

The vertical walls that flank the cavity opening from above and below are adiabatic and are also surfaces of zero velocity. In the external environment at locations sufficiently far from the cavity opening, the temperature is $T_\infty$, and the velocities are vanishingly small. The application of these far-field boundary conditions is not a straightforward matter and may have been mishandled in prior investigations.

In this regard, representative treatments of the far-field boundary conditions in the relevant published literature will be discussed. In one paper, the vertical velocity $v$ was set equal to zero on all the bounding surfaces $AB$, $BC$, and $CD$ of the extended solution domain (Fig. 1). This model totally blocked any fluid from entering the domain across $CD$ and from leaving the domain across $AB$. At one of these boundaries, the temperature was assigned the value $T_\infty$, while the other boundaries were specified as being adia-

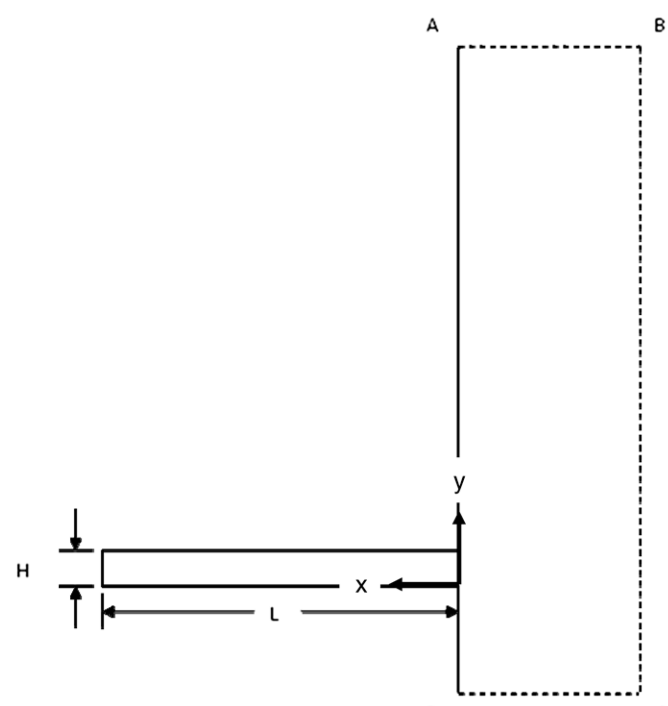


**Fig. 1.** Schematic diagram of the open cavity and the solution domain.